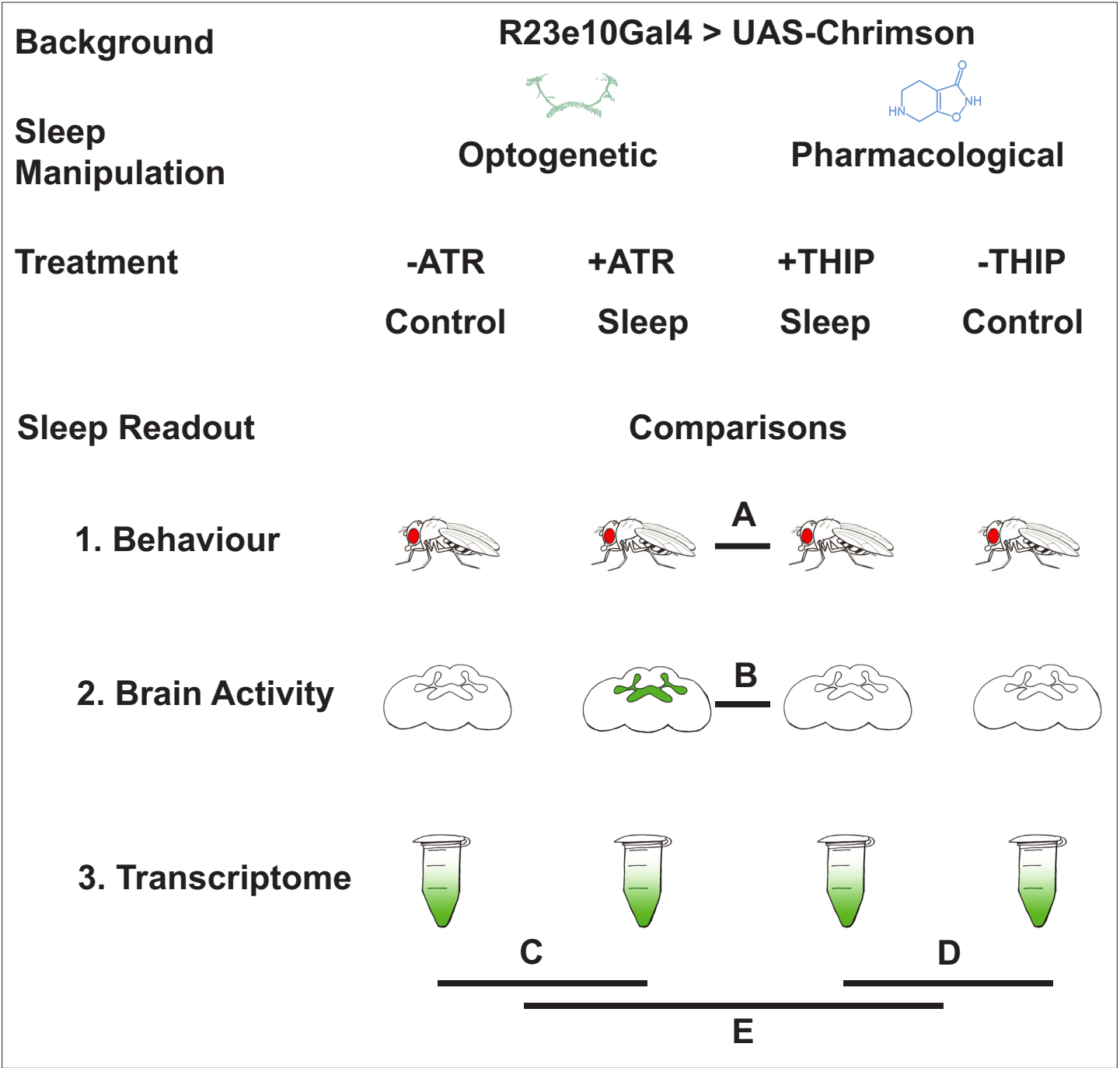

Figures and figure supplements

Experimentally induced active and quiet sleep engage non-overlapping transcriptional programs in *Drosophila*

Niki Anthony et al.



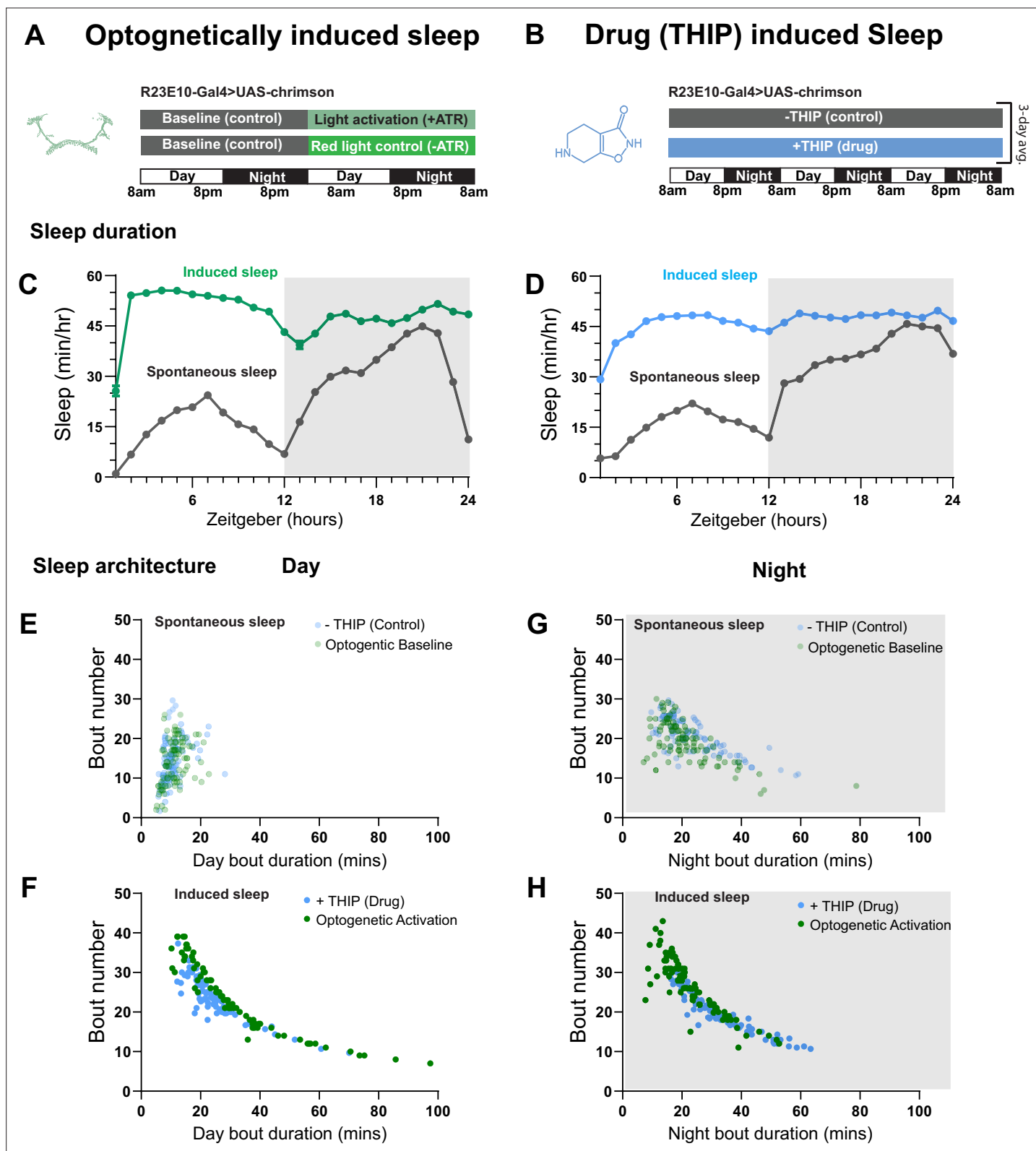


Figure 2. Optogenetic- and 4,5,6,7-tetrahydroisoxazopyridin-3-ol (THIP)-induced sleep have similar effects on sleep duration and consolidation. (A) Experimental regime for observing the effects of optogenetic activation and THIP provision (B). (C) Sleep profile across 24 hr in the baseline condition (gray) and optogenetic activation condition (green). (D) Three-day average of the 24 hr sleep profile of control (gray) and THIP fed (blue) flies. (E) Daytime sleep consolidation scatterplot for optogenetic baseline and THIP control flies. (F) Daytime sleep consolidation scatterplot for optogenetic-
Figure 2 continued on next page

Figure 2 continued

and THIP-induced sleep. **(G)** Night-time sleep consolidation scatterplot for optogenetic baseline and THIP control flies. **(H)** Night-time sleep consolidation scatterplot for optogenetic- and THIP-induced sleep. $n = 87$ for optogenetic activation across three replicates; $n = 88$ for –THIP, $n = 85$ for +THIP, across three replicates. Maximum bout duration possible is 720 min, or 12 hr. See **Supplementary file 1** for statistics.

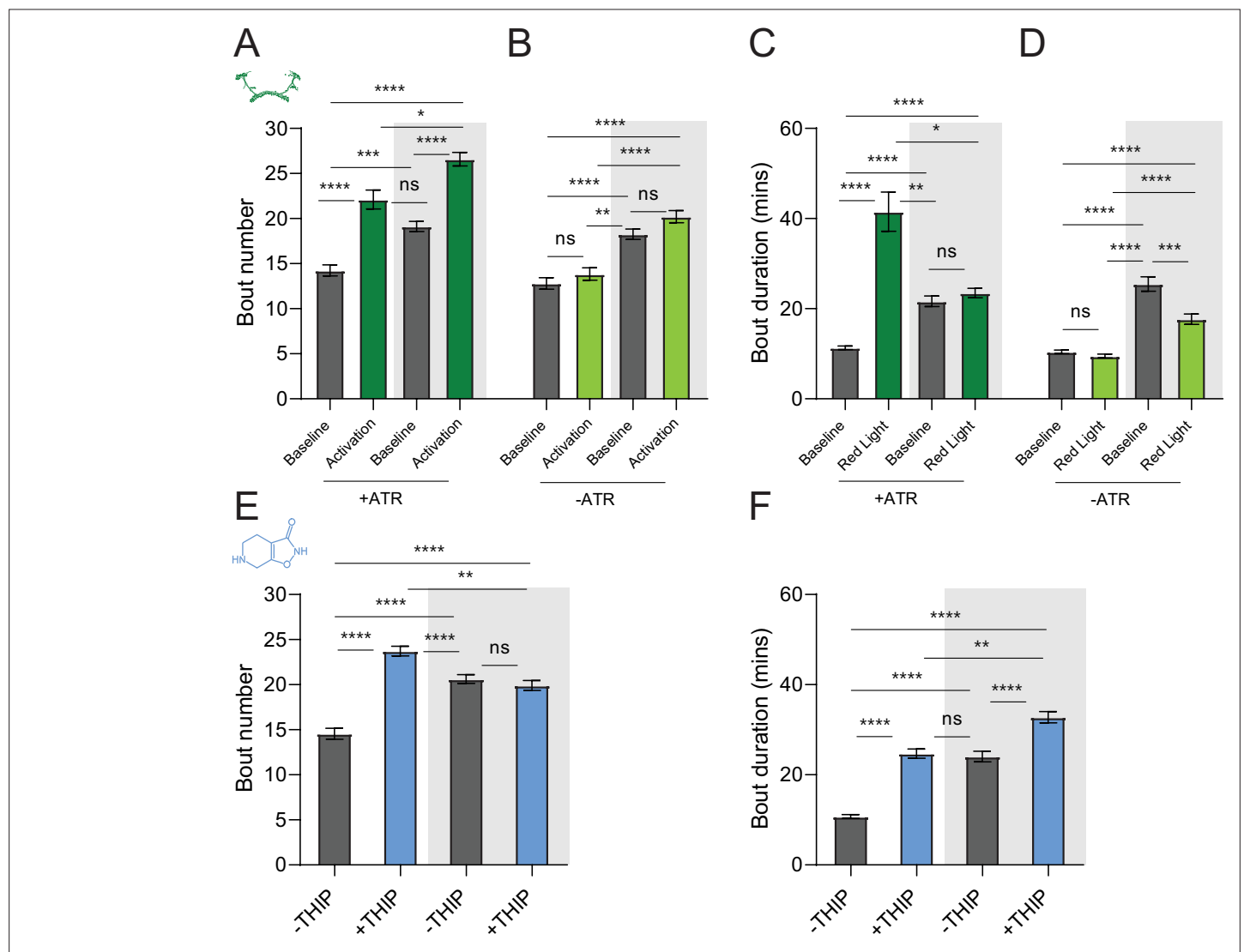


Figure 3. Sleep architecture in optogenetic- and 4,5,6,7-tetrahydroisoxazopyridin-3-ol (THIP)-induced sleep. (A, B) Average number of sleep bouts in control (gray) and optogenetic activation (green) conditions in the day and night for both +ATR (A) and -ATR (B) fed flies. Optogenetic-induced sleep results in an increase in the number of sleep bouts both during the day and the night, whereas red light alone has no effect. (C, D) Optogenetic activation (green) increases the average sleep duration during the day, but not the night when compared to controls (gray) in +ATR flies (C). (D) -ATR flies show no difference in mean sleep bout duration during the day, but show a decrease in average bout duration during the night. THIP (blue) increases both the average number of sleep bouts (E) and the average duration of sleep bouts (F) during the day, but not the night, when compared to controls (gray). Analysis for (A) and (B) = Kruskal–Wallis test with Dunn’s multiple-comparison correction. * $p < 0.05$, *** $p < 0.001$, **** $p < 0.0001$. For (E) and (F), analysis = ordinary one-way ANOVA with Tukey’s correction for multiple comparisons. *** $p < 0.001$, **** $p < 0.0001$.

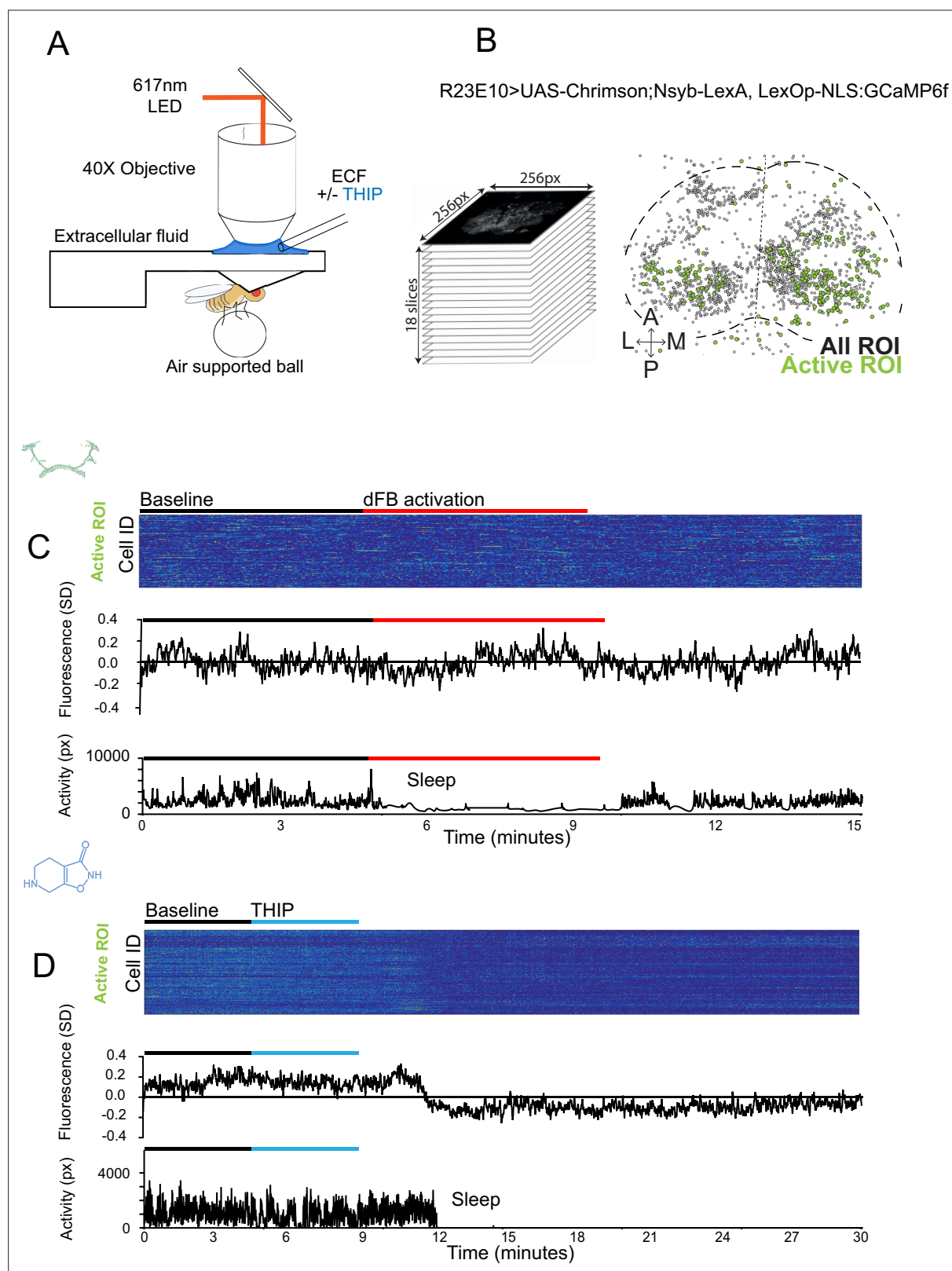


Figure 4. Brain imaging during optogenetic- and 4,5,6,7-tetrahydroisoxazopyridin-3-ol (THIP)-induced sleep. **(A)** Flies were mounted onto a custom-built holder that allowed a coronal visualization of the brain through the posterior side of the head. Perfusion of extracellular fluid (ECF) occurred throughout all experiments. A 617 nm LED was delivered to the brain through the imaging objective during optogenetic experiments. During THIP experiments, 4% THIP in ECF was perfused onto the brain through a custom perfusion system. Behavior was recorded as the movement of flies on

Figure 4 continued on next page

Figure 4 continued

an air-suspended ball. **(B)** Left: imaging was carried out across 18 z-slices, with a z-step of 6 μm . Each z-plane spanned 667 $\mu\text{m} \times 667 \mu\text{m}$, which was captured across 256×256 pixels. Right: a collapsed mask from one fly of neurons found to be active (green) in **(C)** alongside all identified regions of interest (ROIs, gray). **(C)** Neural activity in an example fly brain, represented across cells (top) and as the population mean (middle) did not change following optogenetic-induced sleep (bottom). **(D)** Neural activity in an example fly brain, represented across cells (top) and as the population mean (middle) showed an initial high level of activity in the baseline condition, which decreased when the fly fell asleep (bottom) following THIP exposure. The Y-axis scale is standard deviation of the experiment mean, so the baseline is not absolute but rather reflects any difference with the overall experiment mean.

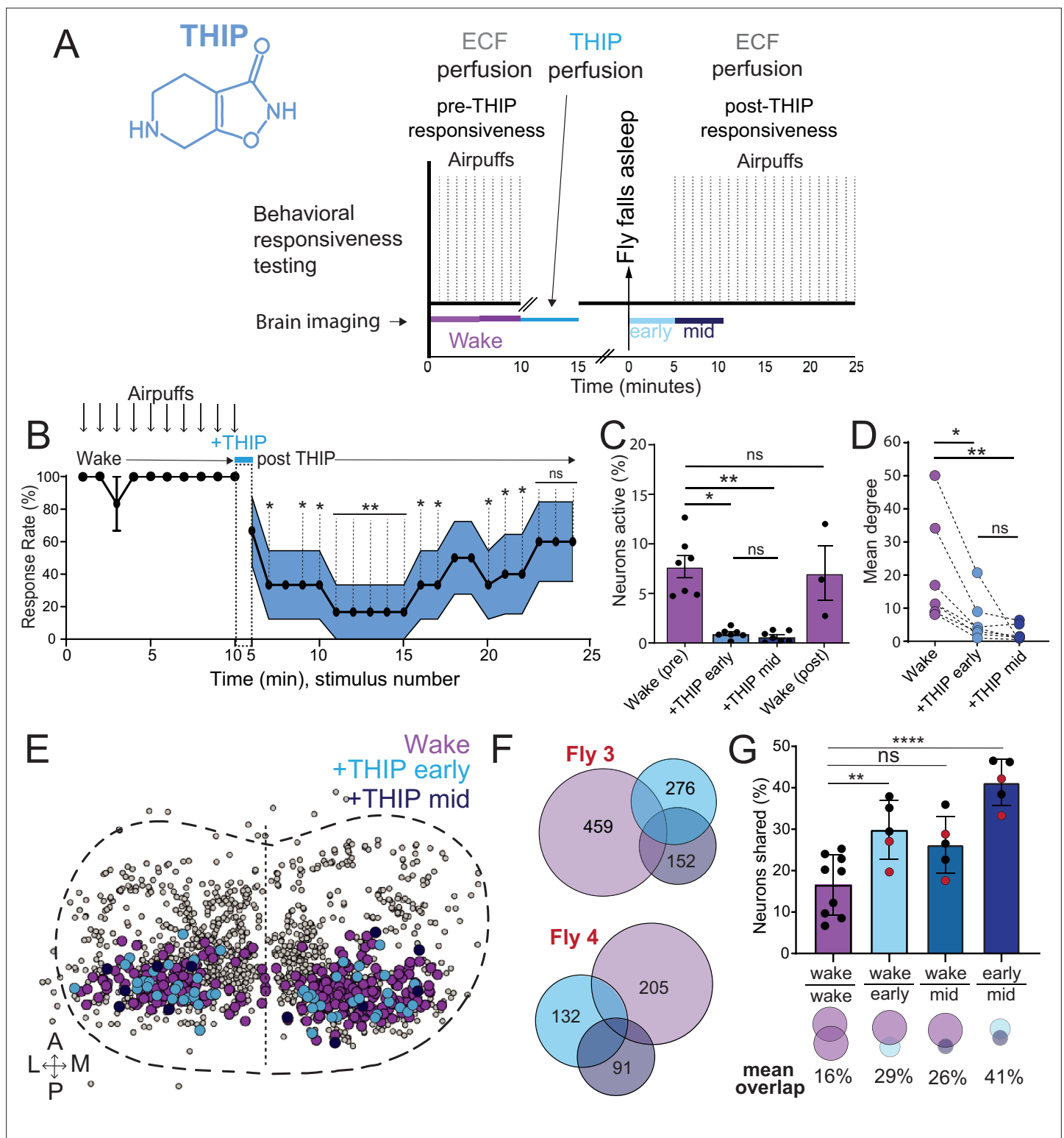


Figure 5. Brain activity and connectivity decrease during 4,5,6,7-tetrahydroisoxazolo[4,5-g]pyridin-3-ol (THIP)-induced sleep. **(A)** Experimental protocol for behavioral responsiveness and brain imaging experiments. 5 min of baseline condition were recorded, during which the exposed brain was perfused with extracellular fluid (ECF), followed by 5 min of THIP perfusion. Following sleep induction, an additional 10 min of calcium activity was recorded, which was separated into 'early' and 'mid' sleep for analysis. Air puff stimuli were delivered to test for behavioral responsiveness. **(B)** Mean behavioral response rate (% \pm SEM) to air puff stimuli over the course of an experiment ($n = 6$). Air puff delivery times are indicated by the solid dots. **(C)** Percent neurons active (\pm SEM) in UAS:Chrimson/X; Nsyb:LexA/+; LexOp:nlsGCaMP6f/R23E10:Gal4 flies during wake, THIP-induced sleep, and recovery ($n =$

Figure 5 continued on next page

Figure 5 continued

9; three flies were recorded post-waking). **(D)** Correlation analysis (mean degree \pm SEM) of active neurons in **(C)**. **(E)** Collapsed mask of neurons active during wake, and both early and mid THIP sleep. **(F)** Overlap in neural identities between wake and THIP-induced sleep in two example flies. Number indicates active neurons within each condition; same color code as in **(E)**. **(G)** Quantification of neural overlap data. Red dots indicate the flies shown in **(F)**. $n = 9$ flies. All tests are one-way ANOVA with Dunnett's multiple-comparison test. ns, not significant, $*p < 0.05$, $**p < 0.01$, $****p < 0.001$.

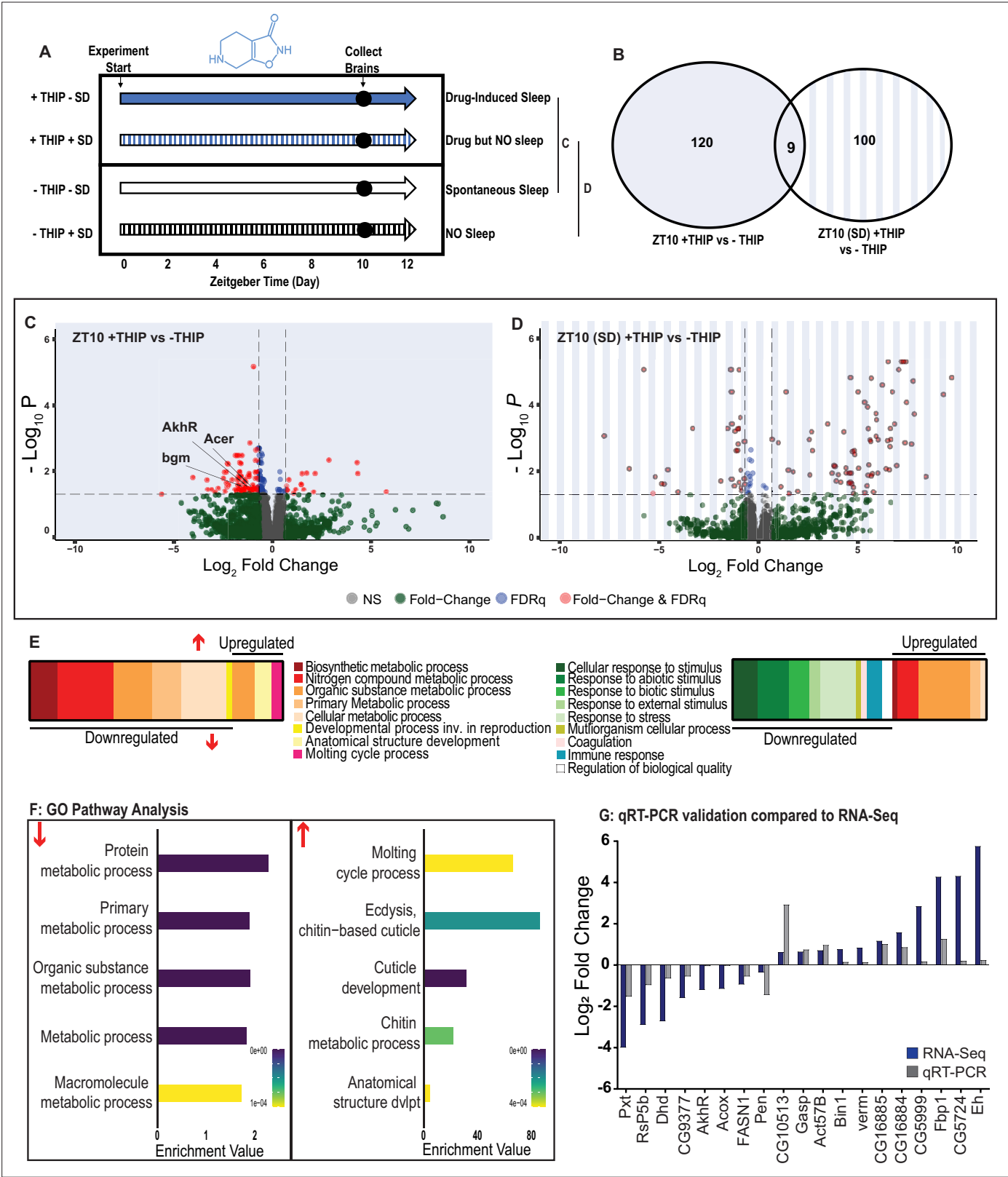


Figure 6. Metabolic processes are downregulated during 4,5,6,7-tetrahydroisoxazopyridin-3-ol (THIP)-induced sleep. **(A)** Schematic representation of the experimental set-up and samples processed using RNA-sequencing. **(B)** Venn diagram showing the gene expression overlap between flies that had been treated with THIP vs. their control (shaded blue) and flies that had been treated with THIP in a sleep-deprived background vs. their control (shaded blue bars). The number of significant differentially expressed genes in each category is indicated. **(C)** Volcano plot representing the distribution

Figure 6 continued on next page

Figure 6 continued

of differentially expressed genes in the presence or absence of THIP. Genes that are significantly up-/downregulated meeting a Log2Fold change of 0.58 and FDRq value of 0.05 are shown in red. Genes meeting the threshold for FDRq value only are shown in blue. Fold change only is shown in green. Those genes not meeting any predetermined criteria are shown in gray. **(D)** Volcano plot representing the distribution of differentially expressed genes in the presence or absence of THIP in a sleep-deprived background. Criteria as above **(C)**. **(E)** Schematic representation of Gene Ontology (GO) enrichment of biological process results. Color coded to indicate parent and child terms for comparisons between groups highlighted above **(C, left, D, right)**. **(F)** Bar chart representation of a subset of interesting significant GO pathway terms originating from the organic substance and primary metabolic processes for the dataset shown in **(C)**. **(G)** Comparison between significant gene hits obtained via RNA-sequencing (blue) and qRT-PCR (gray) in response to THIP, represented by Log2Fold change values. See **Figure 6—figure supplements 1 and 2** and **Figure 6—source data 1 and 2**.

	GO Term	Pvalue	Enrichment value
Downregulated	GO:0046460 neutral lipid biosynthetic process	0.0006	52.92
	GO:0046463 acylglycerol biosynthetic process	0.0006	52.92
	GO:0002181 cytoplasmic translation	0.0000	33.41
	GO:0009059 macromolecule biosynthetic process	0.0000	6.44
	GO:0009058 biosynthetic process	0.0000	4.53
	GO:0009064 glutamine family amino acid metabolic process	0.0008	16.54
	GO:0006412 translation	0.0000	11.7
	GO:0043043 peptide biosynthetic process	0.0000	11.54
	GO:0043604 amide biosynthetic process	0.0000	10.48
	GO:0006518 peptide metabolic process	0.0000	8.89
	GO:1901566 organonitrogen compound biosynthetic process	0.0000	6.38
	GO:0044271 cellular nitrogen compound biosynthetic process	0.0000	5.07
	GO:0034641 cellular nitrogen compound metabolic process	0.0000	2.31
	GO:1901564 organonitrogen compound metabolic process	0.0000	2.06
	GO:0006807 nitrogen compound metabolic process	0.0002	1.6
	GO:1901576 organic substance biosynthetic process	0.0000	4.53
	GO:0019752 carboxylic acid metabolic process	0.0008	3.36
	GO:0043436 oxoacid metabolic process	0.0010	3.26
	GO:0006082 organic acid metabolic process	0.0010	3.25
	GO:0019538 protein metabolic process	0.0000	2.27
	GO:0071704 organic substance metabolic process	0.0000	1.9
	GO:0043170 macromolecule metabolic process	0.0001	1.72
	GO:0006591 ornithine metabolic process	0.0006	52.92
	GO:0006525 arginine metabolic process	0.0008	44.1
	GO:1901605 alpha-amino acid metabolic process	0.0003	6.73
	GO:0008152 metabolic process	0.0000	1.83
	GO:0044238 primary metabolic process	0.0000	1.89
	GO:0019432 triglyceride biosynthetic process	0.0003	66.15
	GO:0006414 translational elongation	0.0000	34.51
	GO:0034645 cellular macromolecule biosynthetic process	0.0000	7.55
	GO:0043603 cellular amide metabolic process	0.0000	7.7
	GO:0044249 cellular biosynthetic process	0.0000	4.69
	GO:0044267 cellular protein metabolic process	0.0000	2.58
	GO:0044260 cellular macromolecule metabolic process	0.0000	2.02
	GO:0044237 cellular metabolic process	0.0000	1.67
Upregulated	GO:0007548 sex differentiation	0.0003	22.05
	GO:0006030 chitin metabolic process	0.0003	21.44
	GO:1901071 glucosamine-containing compound metabolic process	0.0004	19.78
	GO:0006040 amino sugar metabolic process	0.0004	19.33
	GO:0006022 aminoglycan metabolic process	0.0006	17.48
	GO:0018990 ecdysis, chitin-based cuticle	0.0002	85.05
	GO:0022404 molting cycle process	0.0004	65.42
	GO:0040003 chitin-based cuticle development	0.0000	32.89
	GO:0042335 cuticle development	0.0000	31.33
	GO:0048856 anatomical structure development	0.0004	4.39
Metabolic process			
Biosynthetic metabolic process			
Nitrogen compound metabolic process			
organic substance metabolic process			
primary metabolic process			
Cellular metabolic process			
Developmental Process			
Developmental process involved in reproduction			
Anatomical structure development			
Multicellular organismal process			
Molting cycle process			

Figure 6—figure supplement 1. Gene Ontology (GO) enrichment analysis for 4,5,6,7-tetrahyrdoisoxazolopyridin-3-ol (THIP)-induced sleep. Significantly downregulated and upregulated GO categories for THIP-sleep (**Figure 6—source data 1**), listed from most enriched at the top. Broad GO categories are identified below.

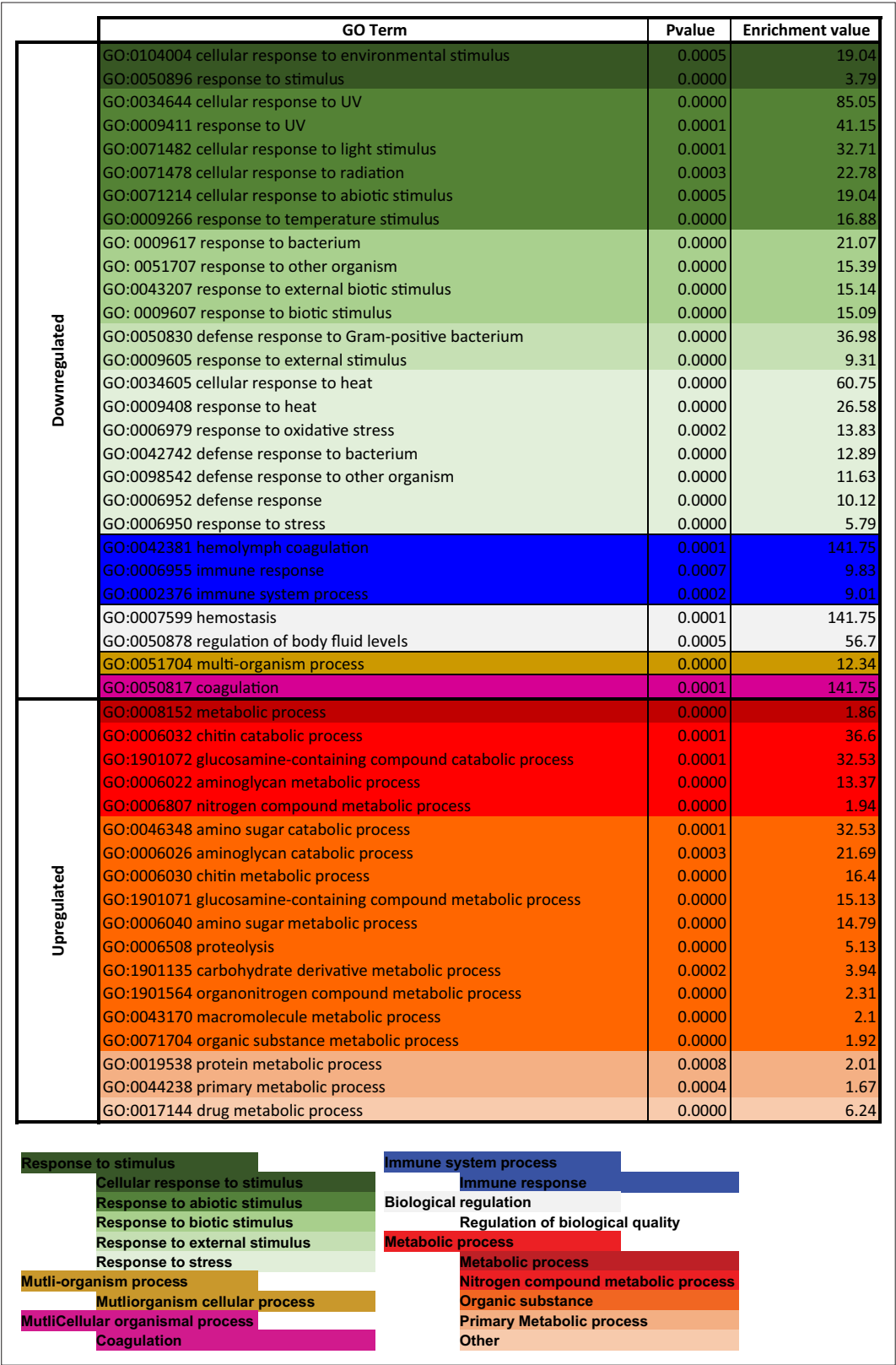


Figure 6—figure supplement 2. Gene Ontology (GO) enrichment analysis for 4,5,6,7-tetrahydoisoxazopyridin-3-ol (THIP)-provisioned flies that were sleep deprived. Significantly downregulated and upregulated GO categories for sleep-deprived flies (**Figure 6—source data 2**), listed from most enriched at the top. Broad GO categories are identified below.

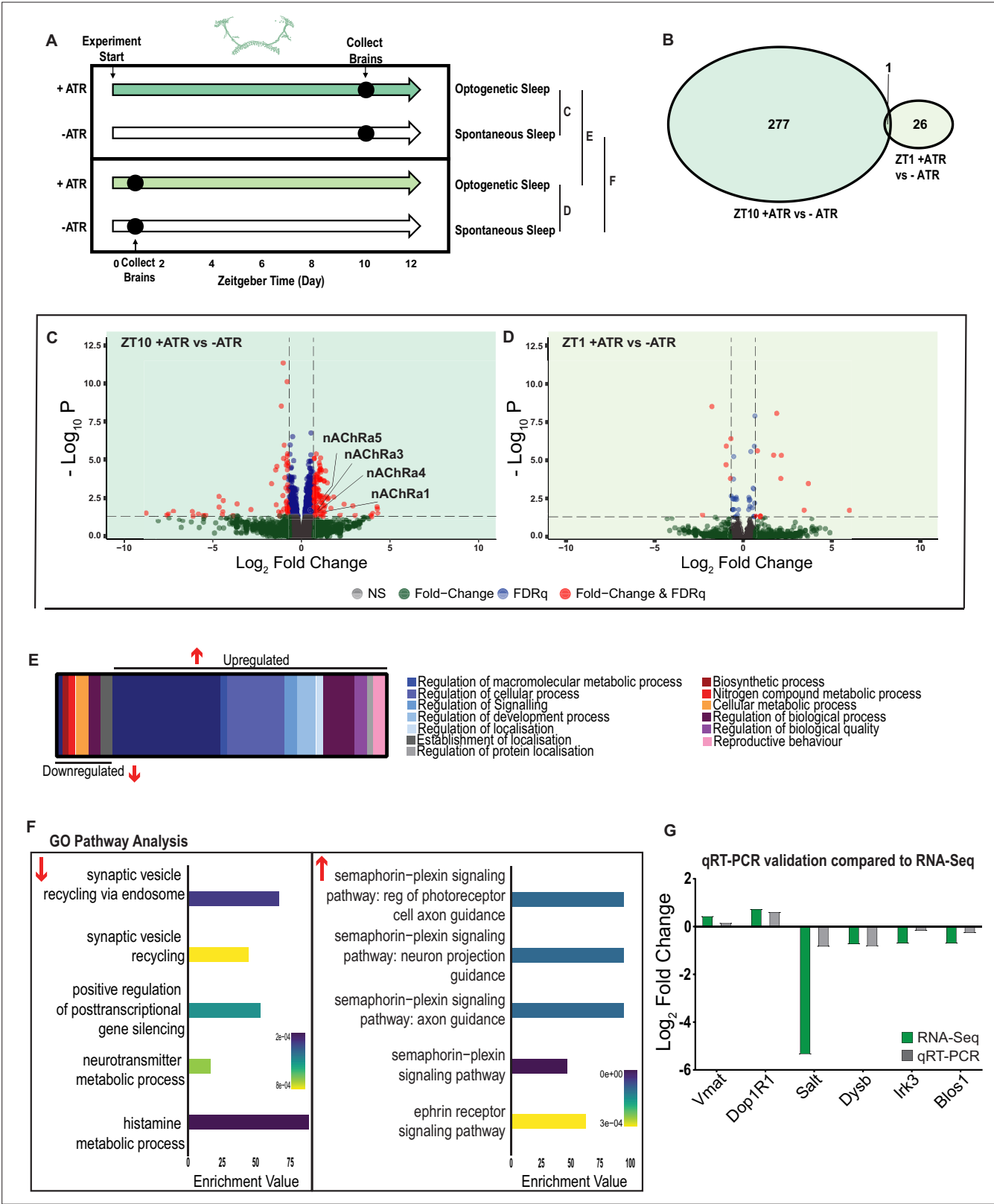


Figure 7. A variety of biological processes including axon guidance are upregulated during optogenetic-induced sleep. **(A)** Schematic representation of the experimental set-up and samples processed using RNA-sequencing. **(B)** Venn diagram showing the gene expression overlap between flies that experienced 10 hr of optogenetic-induced sleep (ZT10) compared to -ATR controls (ZT10) and those flies where optogenetic activation was restricted to 1 hr (ZT1) and compared to -ATR controls (ZT1). **(C)** Volcano plot representing the distribution of differentially expressed genes resulting

Figure 7 continued on next page

Figure 7 continued

from optogenetic activation for 10 hr vs. control flies that were allowed to sleep spontaneously for 10 hr. Genes that are significantly up-/downregulated meeting a Log2Fold change of 0.58 and FDRq value of 0.05 are shown in red. Genes meeting the threshold for FDRq value only are shown in blue. Fold change only in green. Those genes not meeting any predetermined criteria are shown in gray. (D) Volcano plot representing the distribution of differentially expressed genes resulting from optogenetic activation for 1 hr vs. control flies that were allowed to sleep spontaneously for 1 hr. Criteria as above (C). (E) Schematic representation of Gene Ontology (GO) enrichment of biological process results. Color coded to indicate parent and child terms comparing flies that had been activated optogenetically for 10 hr vs. flies that had been allowed to spontaneously sleep for the same duration. (F) Bar chart representation of a subset of interesting significant GO pathway terms originating from the regulation of cellular processes and signaling biological processes. (G) Comparison between significant gene hits obtained via RNA-sequencing (green) and qRT-PCR (gray) in response to optogenetic sleep, represented by Log2Fold change values. See **Figure 7—figure supplements 1–3** and **Figure 7—source data 1–4**.

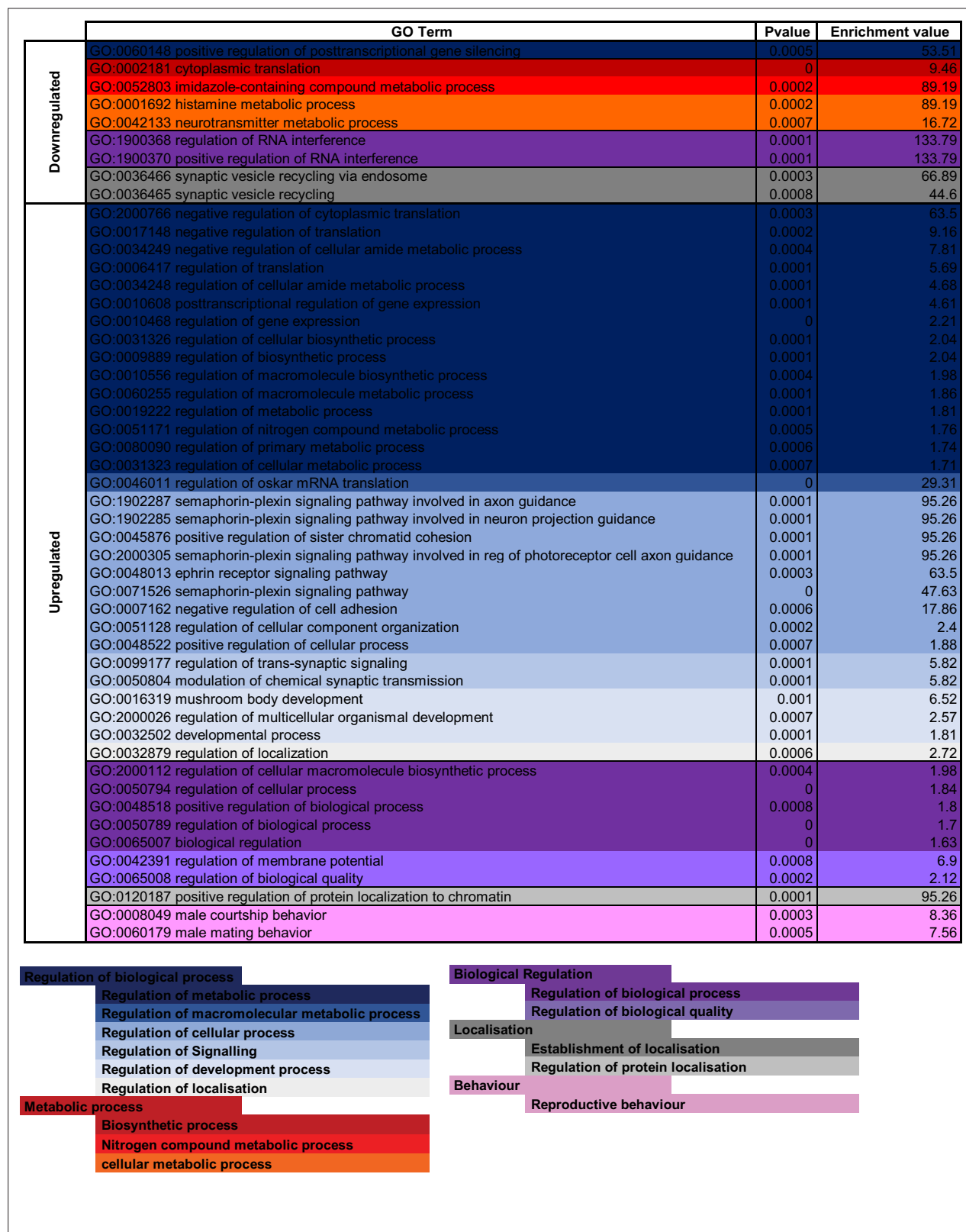


Figure 7—figure supplement 1. Gene Ontology (GO) enrichment analysis for optogenetic-induced sleep. Significantly downregulated and upregulated GO categories for optogenetic-sleep (**Figure 7—source data 1**), listed from most enriched at the top. Broad GO categories are identified below.

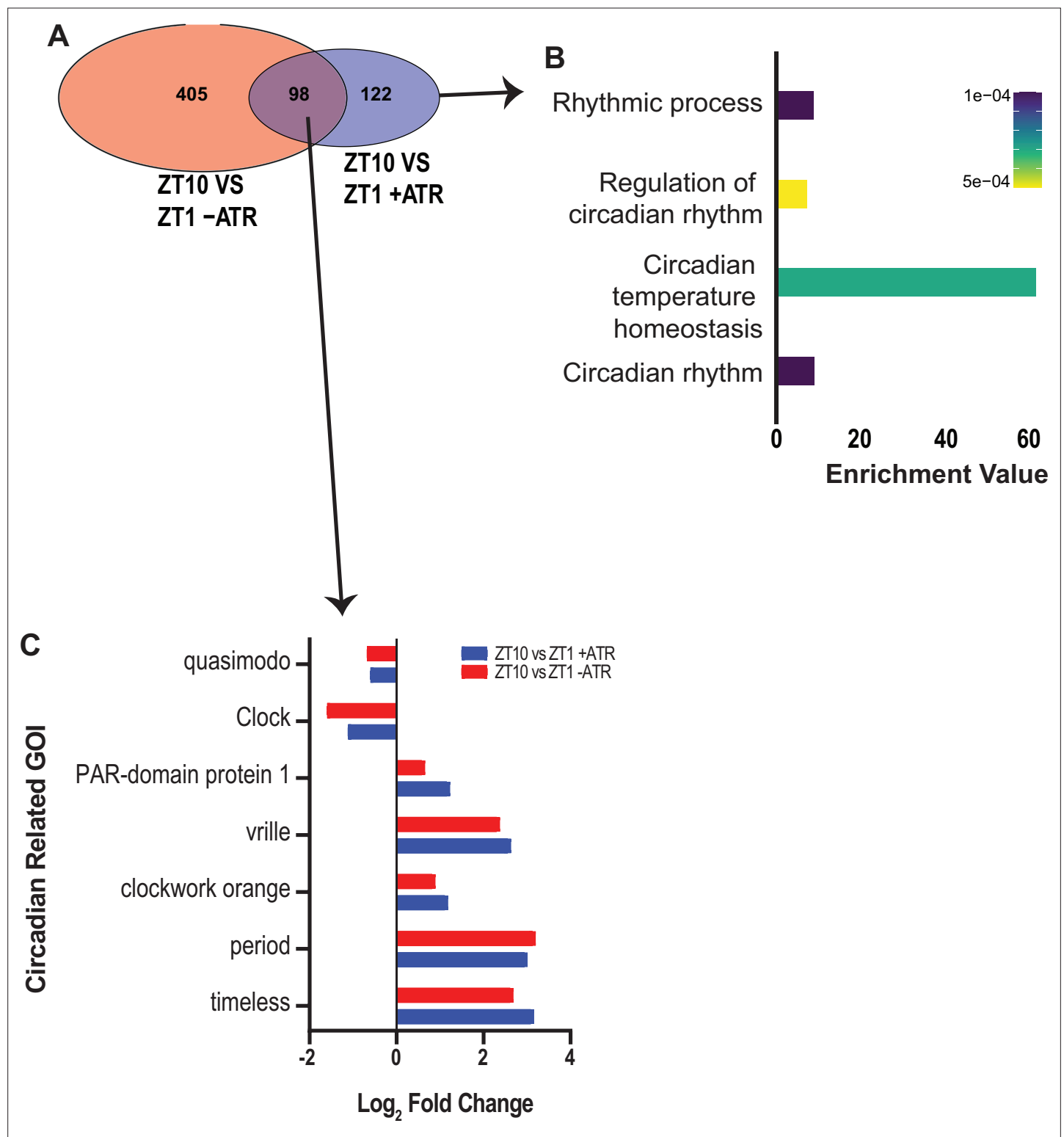
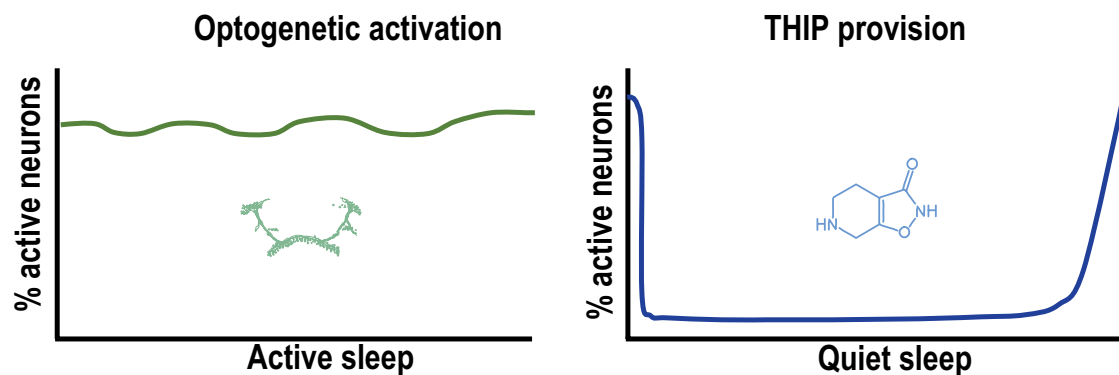


Figure 7—figure supplement 2. Circadian-related genes uncovered in optogenetic-sleep dataset. **(A)** Zeitgeber (ZT) 10 timepoint was compared with ZT to uncover potential circadian-regulated genes in two separate datasets (-ATR and +ATR). A total of 98 genes were shared between these datasets. **(B)** Of the 98 shared genes, circadian-related processes were highly enriched. **(C)** Expression levels of seven circadian genes drawn from the two different datasets in **(A)**.

A: Sleep induction method



B: Induced Sleep Transcriptome: GO Pathways of Biological Processes

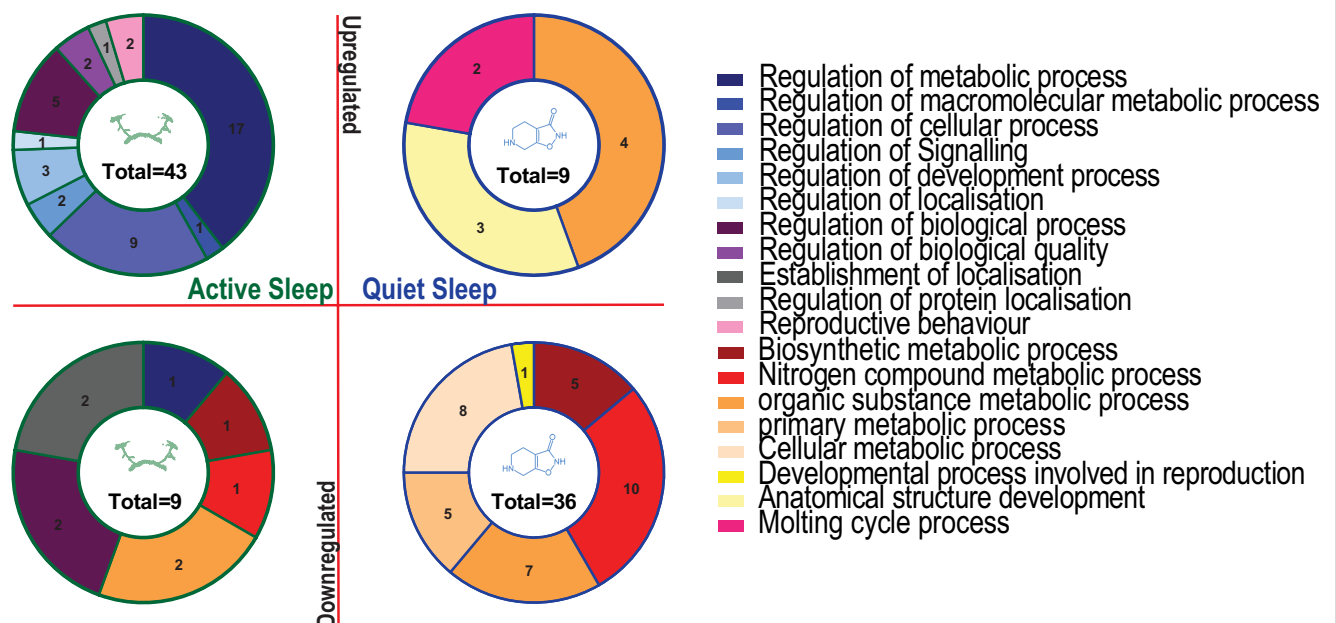


Figure 7—figure supplement 3. Summary of different Gene Ontology (GO) pathways engaged by optogenetic-induced sleep and 4,5,6,7-tetrahydroisoxazopyridin-3-ol (THIP)-induced sleep. **(A)** Either sleep induction method produces different levels of activity in the fly brain. We term optogenetic-induced sleep ‘active sleep’ because brain activity levels are not different than during wake. We term THIP-induced sleep ‘quiet sleep’ because neural activity is significantly decreased already in the first 5 min. Both of these induced forms of sleep resemble sleep stages seen during spontaneous sleep in flies. **(B)** Number of GO pathways engaged by either induced active or quiet sleep, separated by upregulated vs. downregulated biological processes.

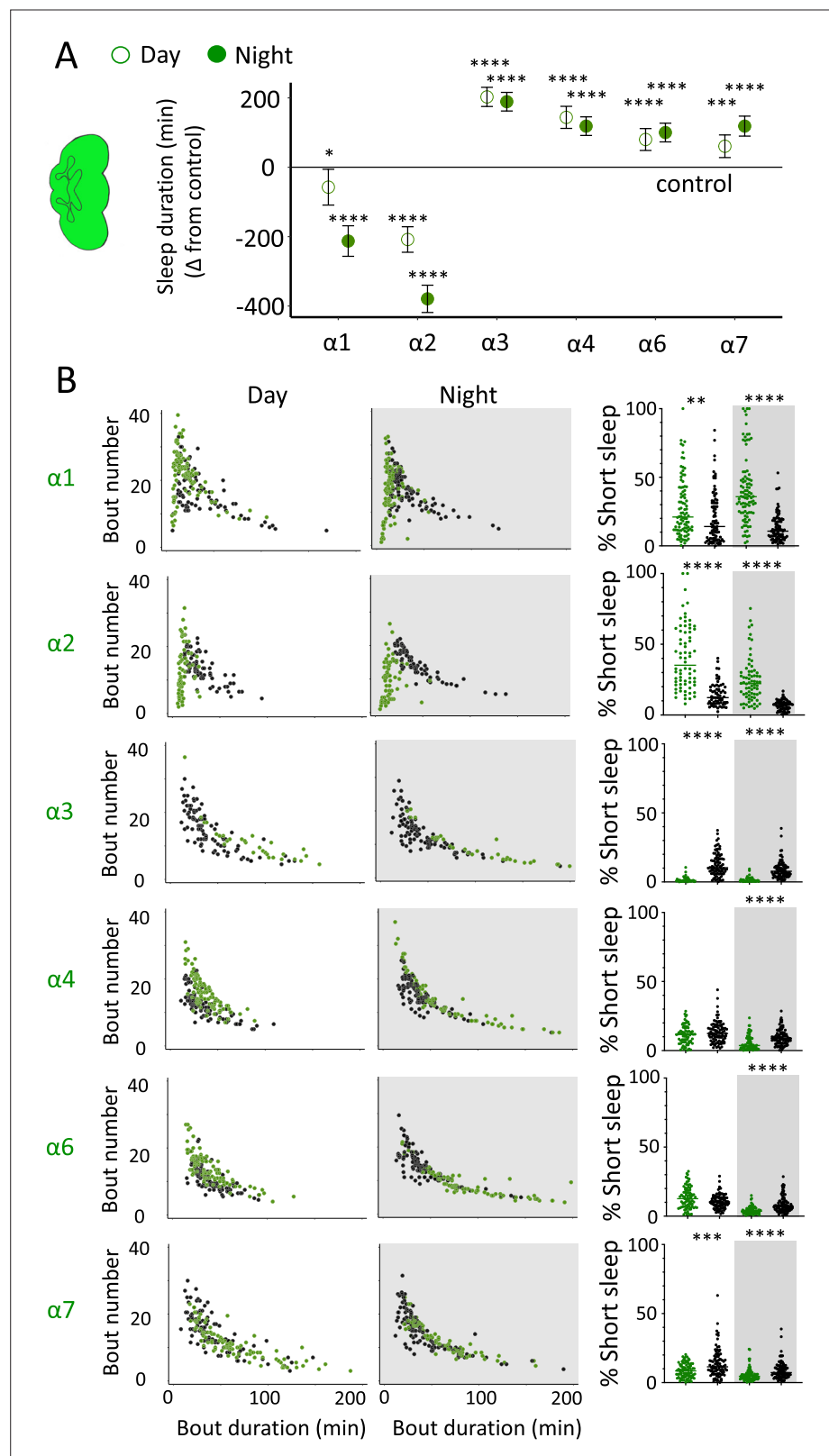


Figure 8. nAChRα subunit knockouts bidirectionally regulate >5 min sleep as well as short sleep. **(A)** Average total day and night sleep duration (minutes ± 95% confidence intervals) in nAChRα knockout mutants, expressed as difference to their respective background controls (see 'Materials and methods'). α1, N = 91; control ($X^{59}w^{118}$) = 93; α2, N = 70; control (w^{118} ActinCas9) = 65; α3, N = 43; (ActinCas9) = 91; α4, N = 87; (w^{118} ActinCas9) = 98; α6,

Figure 8 continued on next page

Figure 8 continued

N = 91; (*w¹¹¹⁸* ActinCas9) = 91; $\alpha 7$, N = 94; (ActinCas9) = 95. * $p < 0.05$, *** $p < 0.001$, **** $p < 0.0001$ by t-test adjusted for multiple comparisons. **(B)** Left two panels: sleep architecture for the same six knockout strains as in **(A)** (green), shown against their respective controls (black). Each datapoint is a fly. Right panels: cumulative short sleep (1–5 min) expressed as a percentage of total sleep duration. Data are from the same experiment as in **(A, B)**. Each datapoint is a fly. ** $p < 0.01$, *** $p < 0.001$, **** $p < 0.0001$ Mann–Whitney *U* test. All data were collected over 3 days and 3 nights and averaged.

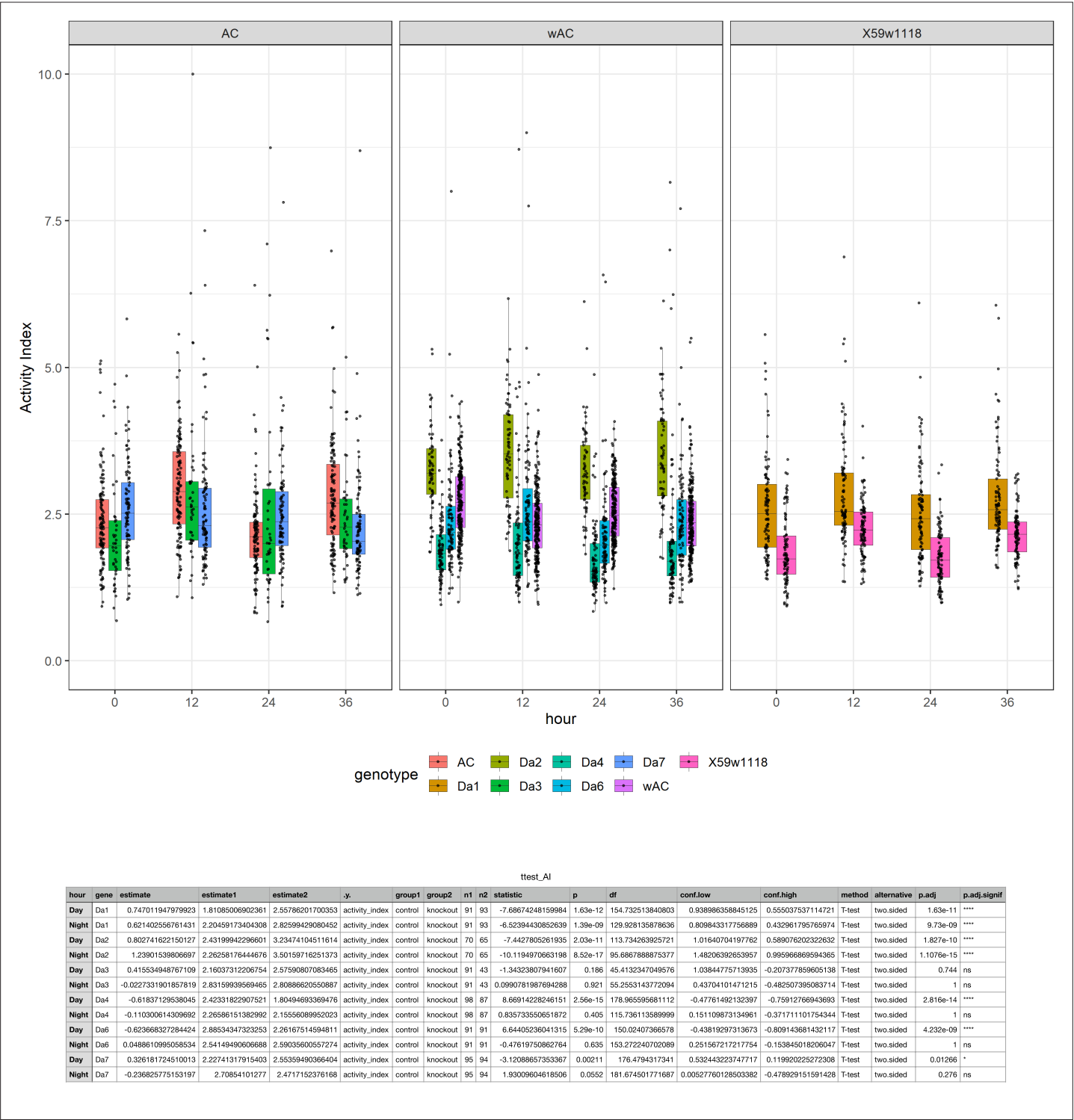


Figure 8—figure supplement 1. Waking activity levels of nAChRα knockout mutants. Top: mutants are compared to their genetic background strain. Da1–7 = nAChRα1–7. Bottom: statistical tests for waking activity levels in each knockout compared to its genetic control, during both day and night.

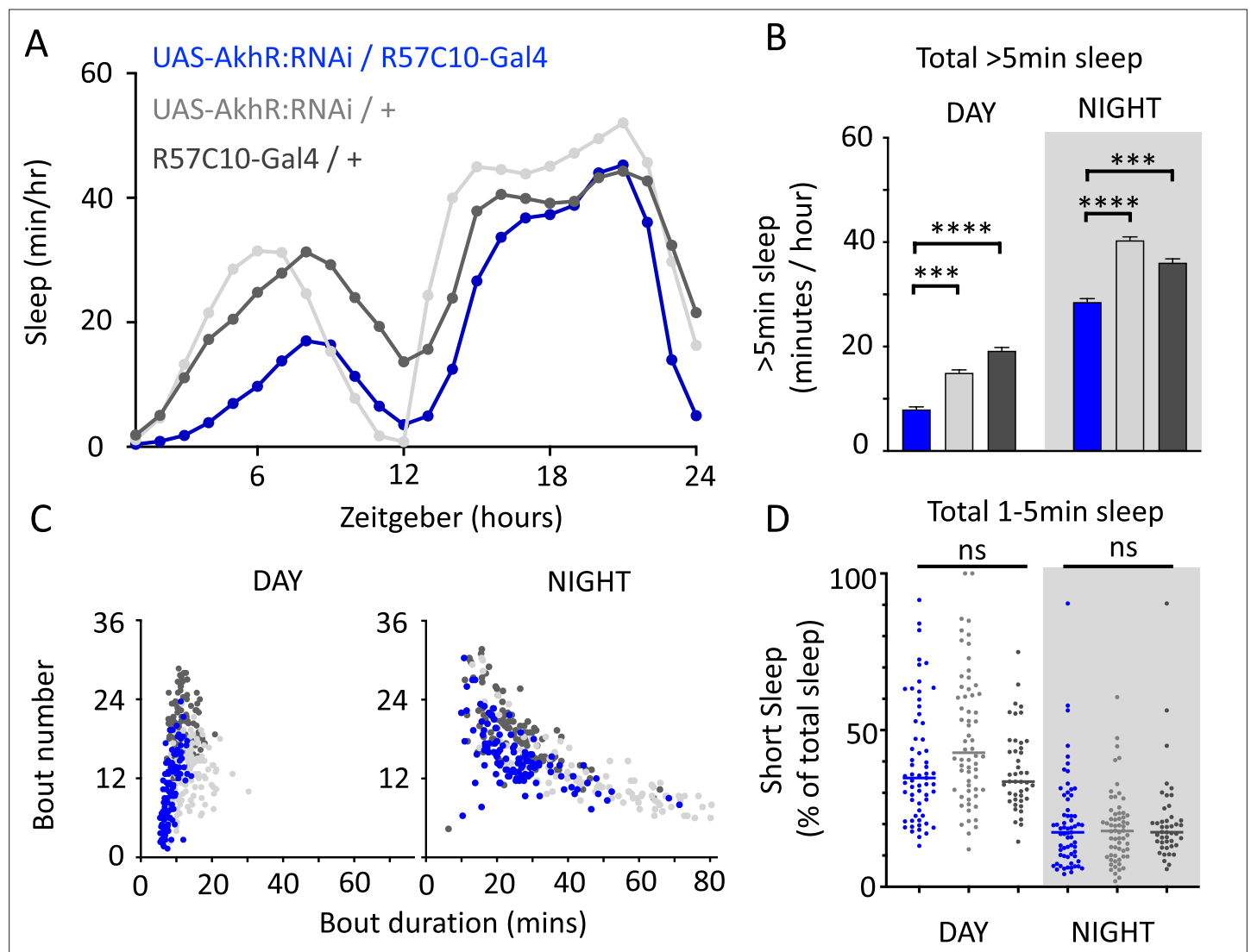


Figure 9. AkhR knockdown decreases >5 min sleep but not short sleep. **(A, B)** Total sleep (>5 min) in UAS-AkhR:RNAi/R57C10-Gal4 flies (blue, N = 126) compared to genetic controls (light gray: UAS-AkhR:RNAi/+, N = 124; dark gray: R57C10-Gal4/+, N = 120). **(C)** Sleep architecture (average bout duration vs. bout number per fly) in data from **(A, B)**. **(D)** Cumulative short sleep (1–5 min, expressed as a % of total sleep) in UAS-AkhR:RNAi/R57C10-Gal4 flies (blue) compared to genetic controls (light gray: UAS-AkhR:RNAi/+; dark gray: R57C10-Gal4/+). Wild-type background (+) is Canton-S(w^{1118}). Each datapoint is a fly. *** $p < 0.001$, **** $p < 0.0001$ Mann–Whitney U test. ns, not significant. All data were collected over 2 days and 2 nights and averaged.

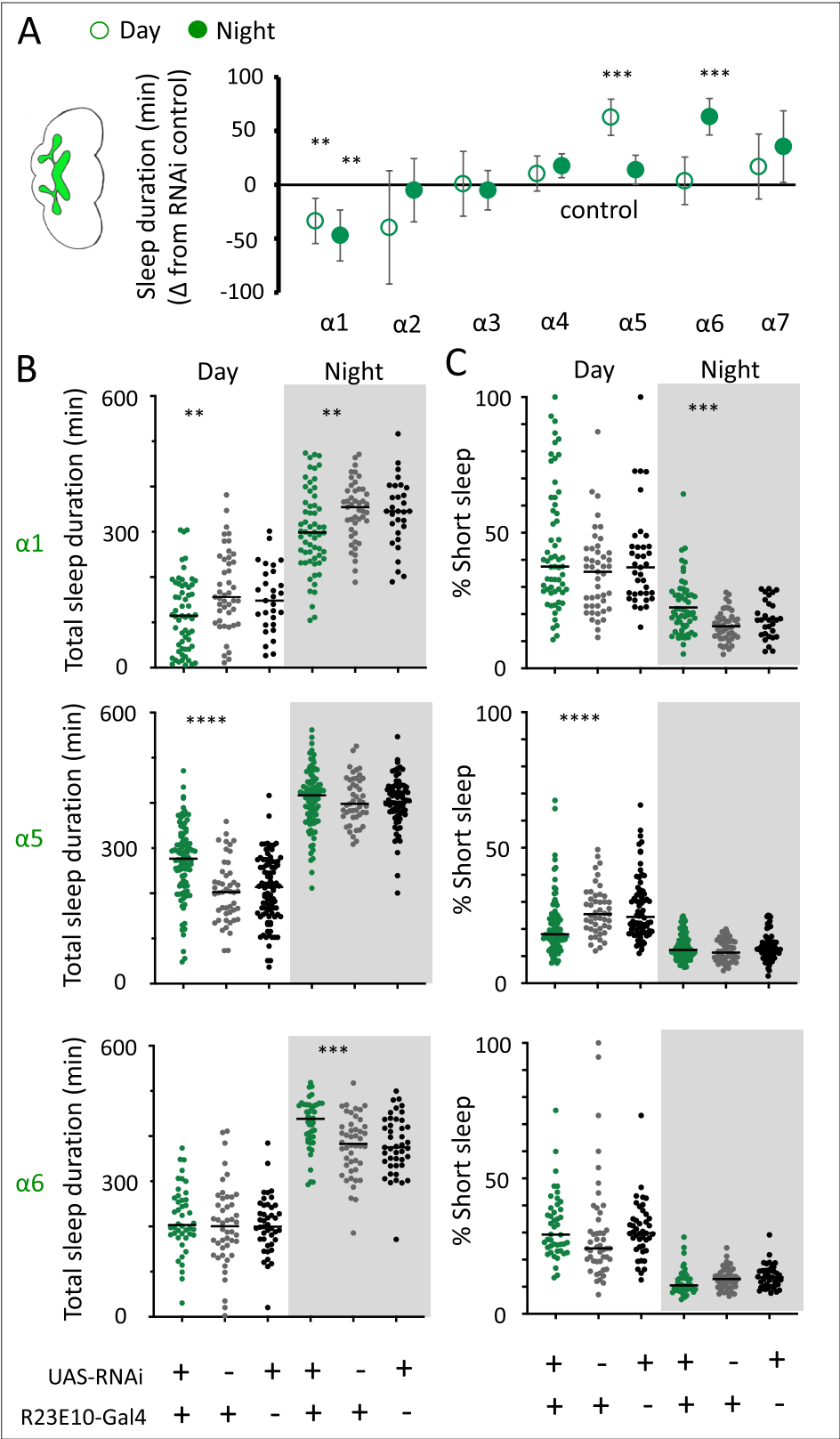


Figure 10. nAChR α subunit knockdowns in sleep-promoting neurons. **(A)** Average total day and night sleep duration (minutes \pm 95% confidence intervals) in UAS-nAChR α RNAi/R23E10-Gal4 flies, expressed as difference to RNAi/+ controls (all were also compared Gal4/+ controls, not shown). $\alpha 1$ N = 60, Gal4 N = 45, RNAi N = 37; $\alpha 2$ N = 21, Gal4 N = 24, RNAi N = 50; $\alpha 3$ N = 33, Gal4 N = 50, RNAi N = 59; $\alpha 4$ N = 92, Gal4 N = 90, RNAi N =

Figure 10 continued on next page

Figure 10 continued

80; $\alpha 5$ N = 94, Gal4 N = 47, RNAi N = 74; $\alpha 6$ N = 44, Gal4 N = 47, RNAi N = 43; $\alpha 7$ N = 32, Gal4 N = 57, RNAi N = 44. ** $p < 0.01$, *** $p < 0.001$ by t-test adjusted for multiple comparisons. **(B)** Total >5 min sleep duration data for significant knockdowns in **(A)**. **(C)** Cumulative short sleep (1–5 min) expressed as a percentage of total sleep duration. Data are from the same experiment as in **(A, B)**. Each datapoint is a fly. *** $p < 0.001$, **** $p < 0.0001$ Mann–Whitney U test. All data were collected over 2 days and 2 nights and averaged.